

Superior plant based carbon fibers from electrospun poly-(caffeyl alcohol) lignin



Mangesh Nar^a, Hussain R. Rizvi^c, Richard A. Dixon^{b, e}, Fang Chen^{b, e}, Adriana Kovalcik^{d, f}, Nandika D'Souza^{a, c, *}

^a Department of Material Science and Engineering, University of North Texas, 1155 Union Circle #305310, Denton, TX, 76203-5017, USA

^b BioDiscovery Institute and Department of Biological Sciences, University of North Texas, Union Circle #305220, Denton, TX, 76203-5017, USA

^c Department of Mechanical and Energy Engineering, University of North Texas, Union Circle #311098, Denton, TX, 76203-5017, USA

^d Institute for Chemistry and Technology of Materials, Graz University of Technology, Stremayrgasse 9, 8010, Graz, Austria

^e US Department of Energy, BioEnergy Sciences Center (BESC), Oak Ridge National Laboratory, Oak Ridge, TN, 37831, USA

^f Competence Centre for Wood Composites and Wood Chemistry (Wood K plus), Altenberger Straße 69, 4040, Linz, Austria

ARTICLE INFO

Article history:

Received 8 August 2015

Received in revised form

16 February 2016

Accepted 18 February 2016

Available online 22 February 2016

ABSTRACT

Plant-sourced carbon has a valuable impact on zero carbon footprint materials for automotive, aerospace, water filtration and other applications. A new lignin, poly-(caffeyl alcohol) (PCFA, also known as C-lignin), has recently been discovered in the seeds of the vanilla orchid (*Vanilla planifolia*). In contrast to all known lignins which are comprised of polyaromatic networks, the PCFA lignin is a linear polymer derived almost totally from caffeyl alcohol monomers linked head to tail into benzodioxane chains via the 'endwise' radical coupling reactions that typify lignification. In this paper we investigate carbon fiber formed from this linear C-lignin and compare it to a Kraft lignin. The PCFA was extracted and electrospun into fibers without additional modification or blending of polymers. Nanoindentation shows an increase in transverse and axial modulus for PCFA carbon by around 250% and 25% respectively as compared to Kraft lignin carbon. Raman spectroscopy results indicate higher graphitic structure for PCFA carbon than that from Kraft lignin, as seen from G/D ratios of 1.92 vs 1.15 which was supported by XPS and TEM results. Size exclusion chromatography indicates a polydispersity index (PDI) for PCFA of 1.6 as compared to 2.6 for Kraft lignin and Zeta potential measurements show higher ionic conductivity for Kraft lignin as compared to PCFA reflecting higher impurities. The results indicate a new bio-source for carbon fibers based on this newly identified linear lignin.

© 2016 Published by Elsevier Ltd.

1. Introduction

Carbon fibers are a high volume, high performance product in applications ranging from carbon fiber reinforced epoxy for aerospace [1] and marine applications [2], electromagnetic interference shielding [3], biomedical applications for regenerative medicine and cancer treatment [4], energy storage devices [5] and water filtration [6]. A major application of carbon fibers is in composites where enhanced strength to weight ratio is obtained over fiberglass reinforced composites. Currently carbon fiber is manufactured predominantly from polyacrylonitrile (PAN) with a small fraction

originating in pitch. PAN-based carbon fiber uses the acrylonitrile monomer which has a high cost. Pitch raw materials are cheaper but the processing involves cleanup leading to high final cost. Pitch from petroleum is preferred over coal pitch from the perspective of raw material clean up, but vacuum cleaning is required to remove volatile matter [7]. To form carbon fibers, wetting of PAN prior to carbonization is employed. Typical carbon yields for PAN-based and pitch-based carbon fibers are about 50–60% and 70–80% respectively [8]. A pre-oxidation step to carbonization has been shown to result in higher carbon yield [9]. Additional graphitization with argon has increased the carbon yield to 80% for PAN fibers [10]. Synthetic polymers such as polyacetylene [11], polyethylene [12], and polybenzoxazole [13] have also been investigated as a potential route for obtaining carbon but the performance of the final products has been found to be inferior to PAN. The high temperature of the PAN process contributes to a larger energy footprint and

* Corresponding author. Department of Material Science and Engineering, University of North Texas, 1155 Union Circle #305310, Denton, TX, 76203-5017, USA.
E-mail address: ndsouza@unt.edu (N. D'Souza).

consequent impact on materials formed from them for carbon footprint calculations. Because of such concerns, the development of a source of carbon fiber based on plant materials is being strongly promoted [14]. Compared to PAN and pitch precursors, lignin is cost effective and has an aromatic structure that is carbon rich for higher carbon yield [15]. There is therefore considerable interest in determining whether lignin can be developed as a cost-effective feedstock for carbon-based applications, potentially as a byproduct of the processing of lignocellulosic liquid biofuels [16].

Among plant resources, lignocellulose is a dominant constituent of plant dry matter, consisting of a complex of cellulose and hemicellulose embedded in lignin. Lignin is the second most abundant natural polymer on earth, produced by oxidative polymerization of *p*-hydroxycinnamyl alcohols (monolignols). Lignins are primarily found in plant secondary cell walls, and are particularly abundant in vascular tissues. The presence of this lignin reduces forage digestibility and hinders agro-industrial processes for generating pulp or biofuels from lignocellulosic plant biomass. There has therefore been considerable attention given to reducing lignin content in plant feedstocks and developing value added products from the lignin itself [17–20].

Lignin consists of a random polyaromatic network of linked phenylpropanoid units along with various functional groups [21]. Lignins are broadly divided into three categories: softwood (gymnosperm), hardwood (angiosperm) and grass or annual plant (graminaceous) lignin [22]. These different classes of lignin are mainly derived from the copolymerization of three *p*-hydroxycinnamyl alcohol monomers known as monolignols. The primary

monolignols (monomers) are *p*-coumaryl, coniferyl and sinapyl alcohols [23]. From Fig. 1A it can be seen that these monolignols differ from each other due to the methoxyl groups attached to the 3 and 5 positions of the aromatic ring.

These monomers give rise to subunits which couple in different percentages to form different classes of lignin. *p*-coumaryl alcohol gives rise to a *p*-hydroxyphenyl (H) subunit, coniferyl alcohol gives a guaiacyl (G) subunit and sinapyl alcohol gives a syringyl (S) subunit (Fig. 1A).

Softwood lignins are mainly derived from the guaiacyl (G) subunit, having low levels of the *p*-hydroxyphenyl (H) and syringyl (S) subunit. Hardwood lignin consists mainly of both (G) and (S) with low level of (H) subunit. On the contrary grass lignin consists of a higher quantity of (H) subunit as compared to (G) and (S) subunits [24]. The random combination of these subunits gives rise to high variability in chain sequences and conformation. However there are characteristic linkages which are found in different percentages due to the combination of these subunits.

Fig. 1B shows the chemical structures of these linkages. There are typically four types of functional groups, phenolic hydroxyl, aliphatic hydroxyl, methoxyl and carbonyl groups, in lignin.. and Table 1 lists the percentage of these linkages in softwood and hardwood lignins [25]. The topology of grass lignin has not been extensively clarified [26].

Recently Chen et al. [27–29] discovered that seed coats of a variety of plant species contain a previously unsuspected class of lignin-like molecule made entirely from caffeoyl alcohol units (essentially G units lacking the methyl group on the 3-oxygen) which are not found in softwood, hardwood or grass lignin. This is termed C-lignin or poly-(caffeoyl alcohol) (PCFA). Fig. 1A shows the chemical structure of the caffeoyl alcohol monomer and its corresponding C subunit. Analysis of the lignin monomer composition of the seed coat of *Vanilla planifolia* and the Brazilian cactus *Melocactus salvadorensis* by thioacidolysis indicates that the lignin is derived almost totally from caffeoyl alcohol monomers; these are linked head to tail into benzodioxane chains via the 'endwise' radical coupling reactions that typify lignification. Interestingly the β -aryl ether units, which are the dominant linkage units found in both hardwood and softwood lignins derived from coniferyl and sinapyl alcohols, were absent, whereas benzodioxanes were the dominant lignin units accounting for over 98% of the identifiable dimeric units in the polymer. Fig. 1B shows the resulting repeated benzodioxane unit.

To isolate lignin from the biomass there are number of industrial and experimental methods that are being employed. The main purpose of these pulping methods is to minimize the degradation of the carbohydrate component. These chemical pulping processes can be classified into alkaline, acidic or neutral. Some of these processes include Kraft, soda, acid sulfite and organosolv pulping each of which results in different structural modifications and degradation.

Kraft lignin, extracted from hardwoods, has been extensively studied as a feedstock for bioresourced synthetic products. It is a high volume waste obtained as a by-product from the pulp and paper industry [30]. To facilitate the melting of the lignin, organic solvent based extraction, chemical treatment or melt blending are employed [31]. The value of lignin as a source for carbon fibers obtained from melt and dry spinning of hardwood Kraft lignin (HKL), softwood Kraft lignin (SKL) and alkali softwood Kraft lignin was first shown by Otani et al. [32]. Sudo used hydrogenation with NaOH using Raney-Ni [33], followed by steam explosion to isolate the lignin and then modification to lower its softening point, thereby facilitating melt spinning of the fibers. However, this method was expensive and a cheaper alternative was attempted using creosote for phenolysis [34]. Although phenolysis improved

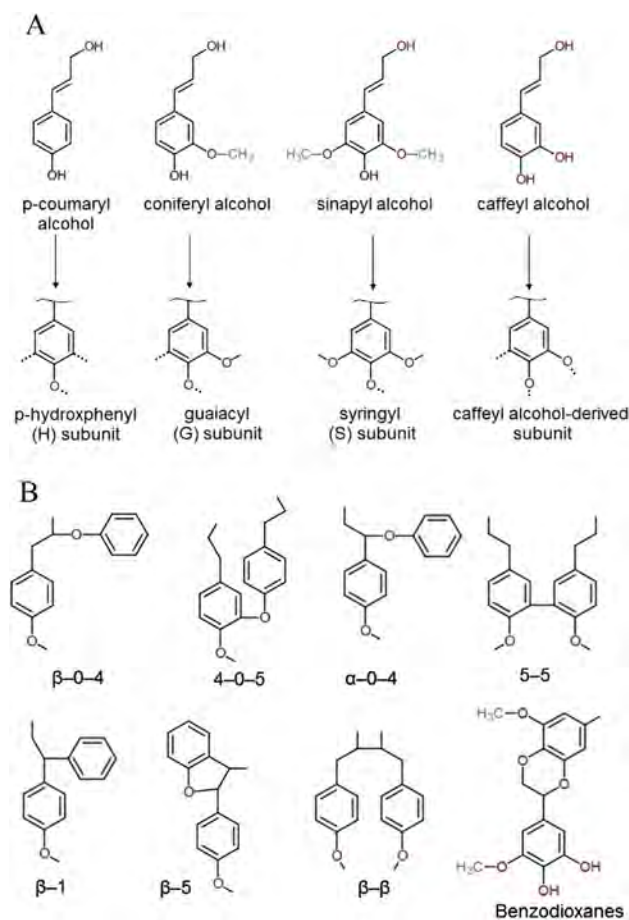


Fig. 1. (A) Lignin monomers and their derived subunits. (B) Common linkages found in lignin structure. (A color version of this figure can be viewed online.)

Table 1
Percentage of linkage types in lignin.

| Linkage type | Dimer structure | % of linkages in softwood | % of linkages in hardwood |
|-------------------|--------------------------------------|---------------------------|---------------------------|
| β -O-4 | Phenylpropane β -aryl ether | 45–50 | 60 |
| 5–5 | Biphenyl and Dibenzodioxocin | 18–25 | 20–25 |
| β -5 | Phenylcoumaran | 9–12 | 6 |
| β -1 | 1,2-Diaryl propane | 7–10 | 7 |
| α -O-4 | Phenylpropane α -aryl ether | 6–8 | 7 |
| 4-O-5 | Diaryl ether | 4–8 | 7 |
| β - β | β - β -linked structures | 3 | 3 |

the yield to 40%, tensile properties were low when compared to hydrogenation. Acetic acid pulping from hardwood gave fusible lignin that could be melt-spun [35]. Lignin from softwood resulted in a high fraction of high molecular weight infusible lignin that must be separated from the fusible fraction in order to facilitate melt spinning [36].

Chemo-enzymatic treatment (sulfonation) [37] has been shown to transform water insoluble Kraft and organosolv lignin to water soluble material, and facilitates grafting of acrylic compounds onto the lignin backbone. Esterification of lignin from sources such as palm trunk, poplar, maize, barley, wheat, and rye with succinate anhydride [38] showed relatively low substitution of succinate, but gave thermal stability ranging from 100 to 600 °C, with the highest for lignin from rye.

Conversion of lignin to carbon fiber has followed many routes. One approach requires modification of the fiber surface during fiber formation through use of a low boiling point solvent such as ethanol in a coaxial die [12]. Switching from Kraft to Allcell lignin has also been employed. Lallave et al. [39] electrospun Allcell lignin (an organosolv lignin that is highly hydrophobic and, unlike Kraft lignin, contains no measurable sulfur and very low ash) into fibers without polymer as a binder, using ethanol in a coaxial needle as an outer sheath to enable fiber formation or using a tri-axial needle with glycerin as a core material and ethanol as an outer sheath.

The second approach uses catalysts such as platinum and a third uses secondary polymers blended in with lignin. Blending polymers with lignin enables fiber integrity through improved melt strength. Poly(ethylene oxide) (PEO) has been widely studied for imparting spinnability into lignin for fiber formation. Incorporation of 3% and 5% PEO in hardwood Kraft lignin (HKL) improved spinning capability and tensile properties, respectively [40,41]. With an Allcell/PEO blend, strong hydrogen bonding resulted in miscible blends aiding spinning of fibers, although the addition of PEO did not improve the mechanical properties of the fiber [42]. To overcome brittleness, lignin was blended with polyethylene terephthalate (PET) and polypropylene (PP). Blends of PET and PP with HKL gave fiber diameter ranges from 30 to 76 μm , and blends with 25% polymers yielded 60% carbon after carbonation [43]. A caveat was that this route did not improve the physical properties of the fibers. Similarly, polyethylene glycol (PEG)-lignin was used for single needle melt spinning by Lin et al. [44] to obtain 23 μm diameter fibers at 170 °C. To electrospin lignin, Ago et al. [45] reported adding 25% of poly(vinyl alcohol) (PVA) to lignin resulting in bead-free uniform diameter fibers. It was also presented that the spinning performance of lignin solution can be improved by its mixing with polyacrylonitrile (PAN) [46,47].

Considerable work remains to be done to obtain carbon from plant sources. In this paper we examine the carbon fiber formed from the recently discovered C-lignin [27–29]. We predict that such a linear structure would enhance the ability to generate carbon fibers by electrospinning. We here test this hypothesis, comparing samples of PCFA from seed coats of *V. planifolia* with Kraft lignin.

2. Experimental

2.1. Materials

Sulfuric acid, 98%, p.a. and tetrahydrofuran, 99.9% were purchased from Carl Roth (Austria). Hydrochloric acid, 37%, was supplied by Sigma Aldrich (Germany).

PCFA (C-lignin) was obtained from seed coats of *V. planifolia*. Vanilla seeds were ground to a powder using a freezer/mill 6870, then extracted with chloroform and methanol three times consecutively. To isolate PCFA, the extracted seeds were mixed with 1% NaOH in a liquid to solid ratio of 10. The mixture was then heated to 120 °C, and the temperature maintained at 120 °C for 1 h in an autoclave. After cooling, the black liquid was separated from the residue by filtration, and PCFA was precipitated from the liquid phase by adjusting the pH to 3.0 with concentrated HCl. The precipitated PCFA was separated by centrifugation, washed with water and freeze dried.

Black liquor (with pH 11.0, total solids 88.9%, Klason lignin 25.1%, and ash 63.8%) was obtained from Zellstoff Pöls AG, Austria, as a by-product during sulfate pulping of 70% spruce, 25% pine and 5% larch. Kraft lignin was isolated from the black liquor by precipitation with 37% HCl. After lowering the pH to 2.0, the precipitated sample was filtered with a Buchner funnel and washed with distilled water twice, to remove unreacted compounds. The filtered sample was purified for 7 days by dialysis against Milli-Q water and subsequently freeze dried.

2.2. Analyses of lignin samples

The purity of Kraft and PCFA lignin was specified by the determination of Klason lignin (acid insoluble lignin), acid soluble lignin and ash according Tappi Standard procedures (T 13 m-54, T 222 om-02, and T 15 os-58).

The composition of non-acetylated lignin samples was determined by C, H, N, S elemental analysis by a Vario El III Universal-Elemental analyzer. Results are presented as average values of two measurements.

The molecular weight averages of lignin samples were determined by size exclusion chromatography (SEC-3010, WGE-DR. Bures instrument equipped with ultraviolet and refractive index detectors). The pure GPC-ORG columns were calibrated using a series of polystyrene standards (Polymer Standard Service). The acetylated lignin samples [48] were dissolved in tetrahydrofuran at a concentration of 4 mg mL⁻¹ and were analyzed at room temperature. Tetrahydrofuran was used as eluent at a flow rate of 1.0 mL min⁻¹ and the injection volume was 100 μL .

2.3. Electrospinning

A 50% solution of PCFA was prepared in 1, 4 dioxane (boiling point of 101 °C). The powder was mixed at 50 °C for 4 h, and then transferred to the syringe for electrospinning at room temperature.

The same process was repeated for Kraft lignin. A 5 ml syringe (National Scientific, Model #57510-5) with an 18 gauge (1.27 mm) 1" long stainless steel blunt needle with a Luer polypropylene hub was used. The syringe with needle was placed on a Razel syringe pump (Model #R99-FM, Razel Scientific Instruments, St. Albans, VT).

The syringe pump flow rate was adjusted to 2.65 ml h⁻¹, to have a continuous flow of solution through the tip of the needle i.e. any bead of solution wiped from the tip is immediately replaced by another. The voltage was increased slowly to observe the drops attracting to the collector until a uniform Taylor's cone was observed and fixed at 20 kV. Distance between the needle and the collector was initially set 10 cm, which gives a wagging stream; this was overcome by increasing the distance to 20 cm for a uniform and aligned stream from the tip of the needle. To form fibers, the solution was pumped from the syringe following which the needle was charged to the prescribed voltage using a high voltage power supply (Model #ES30P-5W/DAM, Gamma High Voltage Research Inc., Ormond Beach, FL). The collector plate was set at the prescribed distance from the needle, covered with non-stick aluminum foil, and grounded. As the syringe pump and the high voltage power supply were switched on, the lignin solution came out of the needle forming a Taylor cone that was attracted by the electrostatic force towards the grounded collector plate.

2.4. Environmental scanning electron microscopy (ESEM)

A FEI Quanta Environmental Scanning Electron Microscope (ESEM; FEI Company, Oregon, USA) was used to image the burnt PCFA and Kraft lignin fibers at an accelerating voltage of 12.5 kV at 10 mm working distance. The samples were sputter coated with gold-palladium to make them conductive and make imaging possible.

2.5. Carbonization

The conditions for thermal stabilization of PCFA and Kraft fibers selected based on our experimental survey and literature were the following [49]: heating from room temperature to 300 °C at a heating rate of 1 °C min⁻¹ for 60 min in an air forced laboratory oven by cascade TEK. The stabilized fibers were then carbonized in Carbolite HZS 12/600 Horizontal Tube Furnace with an alumina tube having an internal diameter of 3–5/8" and outer diameter of 4". The heating rate during the carbonization step was 5 °C min⁻¹. Fibers were held at 900 °C for 45 min under a flow of nitrogen of 0.5 standard cubic feet per hour (SCFH).

2.6. Raman spectroscopy

A 532 nm intensity laser was used at 25% power with aperture of 10 μm slit and objective lens with 10X zoom; this gave a spot size of 2.1 μm. The scan was done from 750 to 2000 cm⁻¹. The exposure time was 15 s and background and sample exposure was performed five times. Background was collected before every sample. This background was subtracted from the Raman spectroscopy results and a baseline correction was performed.

2.7. Nanoindentation

Mechanical properties of Kraft and PCFA were measured along the axial and transverse direction of the electrospun fiber using MTS nanoindenter XP. Samples for the nanoindentation test were prepared by embedding carbonized fibers in an epoxy resin (EPO-FIX Embedding Resin Kit by Electron Microscopy Sciences). CSM (Continuous Stiffness Measurement) method for standard hardness

and modulus with a diamond Berkovich tip was used for indentation [50]. In order to eliminate the effect of environmental noise, a combination of a minus k vibration isolation table and a thermal vibration isolation cabinet was used. Prior to the test, the equipment was tested for calibration on a fused silica reference sample. Eight indents each, in axial and transverse direction on randomly selected Kraft and PCFA carbon fibers, were made. Loading and depth curve obtained from nanoindentation were investigated as defined by Oliver and Parr [51,52]. Reduce Modulus depending upon the slope of the unloading curve $S = \frac{dP}{dh}$ (stiffness), contact area A_c which is a function of indentation depth and geometry of the indenter was calculated using the following equation.

$$E_r = \frac{\sqrt{\pi}}{2\beta} \frac{S}{\sqrt{A_c}} \quad (1)$$

where β is the geometry constant, for Berkovich tip $\beta = 1.034$. Elastic modulus of the fiber E_f is given as a function of Reduce Modulus and mechanical properties of the indenter, according to the following relation.

$$\frac{1}{E_r} = \frac{1 - \nu_f^2}{E_f} + \frac{1 - \nu_i^2}{E_i} \quad (2)$$

where ν_f is the Poisson ratio of the fiber (assumed to be 0.3 for both Kraft lignin and PCFA), E_i is the elastic modulus of the diamond indenter and ν_i is the Poisson ratio of the indenter having values of 1141 GPa and 0.07 respectively.

2.8. Zeta potential

Samples for measurement of Zeta potential were prepared using the cryomilling technique. The PCFA and Kraft lignin were milled using a freezer mill as describe above. The milling was carried out for 15 min to obtain fine powder. A Delta NanoC particle analyzer from Beckman Coulter was used to determine Zeta potential. The dispersions of the PCFA powder and Kraft lignin were made in deionized water at room temperature with sonication for 1 h.

2.9. X-ray photoelectron spectroscopy (XPS)

The chemical structure of Kraft and PCFA carbon fiber was analyzed by X-ray photoelectron spectroscopy (XPS) using a monochromatic 1486.6 eV Al K α radiation with a PHI 5000 VersaProbe (Physical Electronics, Chanhassen, MN). Initially the low resolution survey was performed to identify the elements present on the surface. Then high resolution C1s regions were analyzed to get the binding characteristics of the fiber surface. Shirley background and Gaussian–Lorentzian functions were used for peak fitting.

2.10. Transmission electron microscopy (TEM)

TEM samples were prepared using a dual beam FIB-scanning electron microscope (FEI Nova 200 NanoLab) system with a Ga⁺ ion source. Firstly, a layer of platinum was deposited on the surface for protection, then coarse and medium milling was performed until the sample thickness reached around 1 μm. Next, the Omni probe was used to lift the sample and attach it to the TEM half grid for fine thinning of the sample. TEM imaging was performed using the Tecnai G2 F20 field-emission Scanning Transmission Electron Microscope (S/TEM) operating at 200 kV.

2.11. X-ray diffraction (XRD)

To measure the crystallite size, interplanar spacing and degree of graphitization of carbon fiber from Kraft and PCFA X-ray diffraction was performed using a Rigaku model D/Max–Ultima III (Rigaku Tokyo). X-rays were generated at 44 mA current and 40 kV voltage with Cu K α wavelength (λ) of 1.542 Å. Diffractograms of PCFA and Kraft Carbon fiber were recorded at room temperature in an angular 2θ range of 10–50° with a step size of 0.05 and a scanning rate of 2°/min.

2.12. Thermogravimetric analysis (TGA)

TGA experiments were conducted in an inert environment of argon having a flow rate of 60 ml/min. Samples were heated from room temperature to 800 °C with a heating rate of 10 °C/min to observe thermal stability of each fiber. Experiments were carried out on STA 449 F3 Jupiter from Netzsch.

3. Results and discussion

3.1. Composition of lignins

The amounts of carbon, hydrogen, nitrogen, sulfur, Klason lignin, acid soluble lignin and ash for PCFA and Kraft lignin are listed in Table 2. The PCFA preparation shows about 13.8% higher total lignin content and about 4.8% higher ash content than Kraft lignin. The higher total lignin content means lower content of other non-lignin admixtures such as carbohydrates and extractives present in the PCFA preparation. Lignin derived from one-year-old herbaceous tissues typically contains higher ash content than lignin derived from mature wood due to the high concentration of minerals (silicon, aluminum, calcium, magnesium, potassium and sodium) [53]. The elemental analysis showed 52.9% of carbon, 6.4% of hydrogen, 13.5% of nitrogen and 8.7% of sulfur present in PCFA. In comparison with Kraft lignin, the PCFA preparation contains a lower percentage of carbon, hydrogen and oxygen (oxygen content = 100 – carbon – hydrogen – nitrogen – sulfur – ash) but a higher percentage of nitrogen, sulfur and ash. The higher ash content indicates a higher presence of an inorganic fraction in the seed-derived PCFA preparation than is typical for lignin derived from stem tissues [54]. The detected differences in the elemental compositions of the two lignin preparations are associated with their origins and the applied isolation methods [55].

The molecular weight distributions of acetylated PCFA and Kraft lignin are shown in Fig. 2 and tabulated in Table 3. PCFA lignin exhibited 1.76-fold lower weight-average molecular weight with a narrower weight distribution (\overline{M}_w = 1700 and PDI = 1.6) than Kraft lignin with (\overline{M}_w = 4700 and PDI = 2.6). The narrower molecular weight distribution indicates the higher molecular uniformity of PCFA lignin, which favors its use for fiber applications.

3.2. Electrospun fibers

Solutions of both PCFA and Kraft lignin are electrospinnable. Continuous electrospun fibers were obtained under conditions of

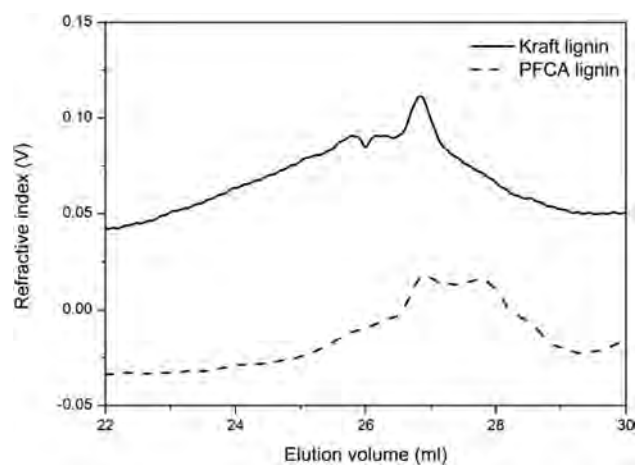


Fig. 2. SEC chromatogram of Kraft and PCFA lignins.

Table 3
SEC characterization of lignins.

| Sample | \overline{M}_n | \overline{M}_w | Polydispersity index (PDI) |
|--------------|------------------|------------------|----------------------------|
| Kraft lignin | 1830 | 4740 | 2.6 |
| PCFA lignin | 1040 | 1700 | 1.6 |

20 kV and 2.65 cc/h solution flow rate with a distance of 20 cm to the stationary collector plate. The conditions were selected as the common conditions that enabled both lignins to form fibers after examining voltages from 5 to 35 kV, distances of 20–40 cm (in increments of 5) for both lignins at the same flow rate. The preliminary ranges were similar to those we employed in a polysaccharide fiber electrospinning investigation [56]. The ESEM images suggest that the fibers obtained are highly uniform with no beads. Obtaining bead-free fibers depends on the conductivity of the solution which elongates the Taylor cone formed at the tip of the needle to give electrospun fibers. During electrospinning of both PCFA and Kraft lignin a minimum voltage of 20 kV was essential to overcome the surface tension of the Taylor cone. A 50% solution in 1,4 dioxane at 50 °C provided enough entanglement in PCFA to spin it into fibers.

The ESEM images (Fig. 3) were analyzed using ImageJ® software. The images were corrected for the scale from pixels of the original tiff image to the known distance on the image to calibrate for scale. A total of 58 measurements of diameters were made and the histogram was plotted for the most frequent occurrence of the diameter range. PCFA produced fine uniform fibers and processed unceasingly compared to Kraft lignin which could only electrospin for a short period (approximately 50.8 mm length compared to continuous spinning for PCFA) prior to fracture (Fig. 4). The diameters of the electrospun fibers from PCFA and Kraft lignin were in the range of 10.5–14 μ m and 30–40 μ m, respectively. The viscosity of the two source solutions entering the syringe pump was determined to be 5333 mPa s for Kraft lignin and 4267 mPa s for PCFA solutions at 12 rpm using a Brookfield viscometer in conjunction with a Spindle # 27.

Table 2
Values of lignin content based on solid residue and elemental analysis.

| Sample | Klason lignin (%) | Acid soluble lignin (%) | ^a Total lignin (%) | Ash content (%) | C (%) | H (%) | N (%) | S (%) |
|--------------|-------------------|-------------------------|-------------------------------|-----------------|-------|-------|-------|-------|
| Kraft lignin | 71.5 | 5.3 | 76.8 | 1.7 | 62.4 | 7.9 | 2.9 | 1.9 |
| PCFA | 76.8 | 13.8 | 90.6 | 6.5 | 52.9 | 6.4 | 13.5 | 8.7 |

^a Total lignin was calculated as Klason + acid soluble lignin.

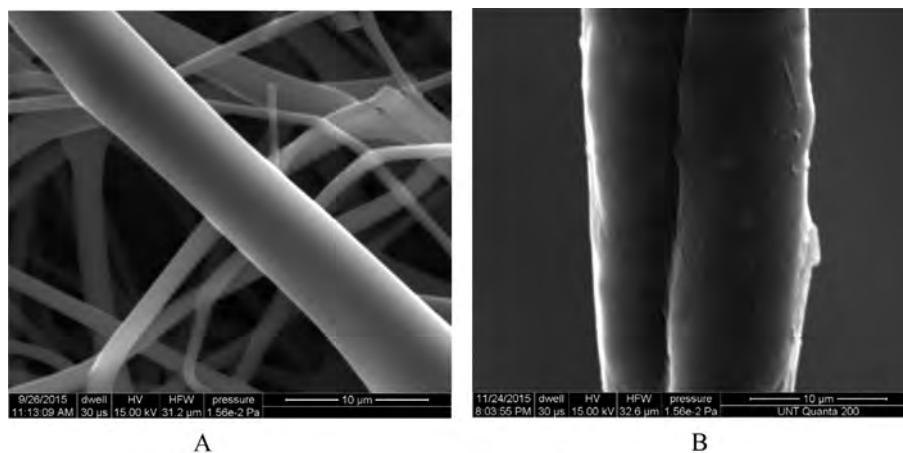


Fig. 3. ESEM image of electrospun carbon fibers. (A) Kraft, (B) PCFA lignin.

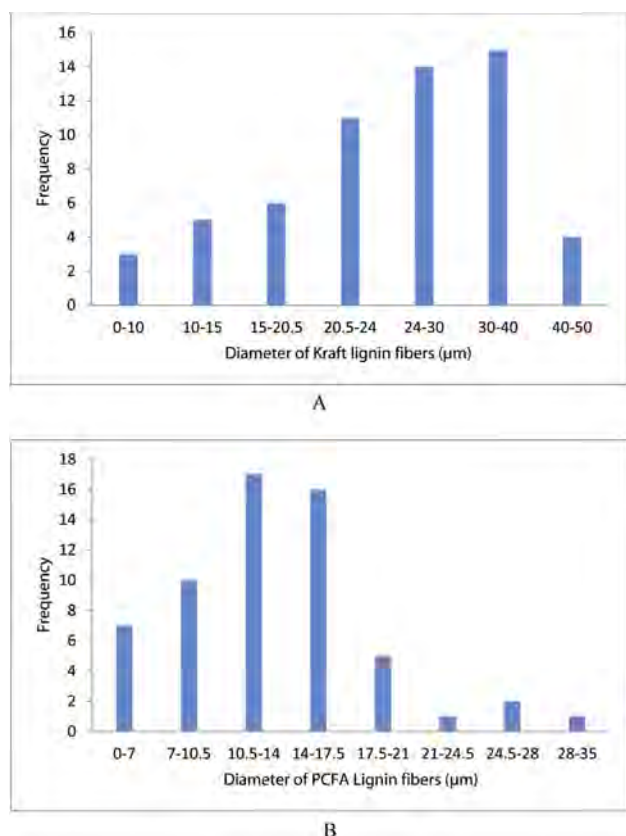


Fig. 4. Histogram of the diameters of electrospun carbon fibers. (A), Kraft, (B) PCFA lignin. (A color version of this figure can be viewed online.)

3.3. Zeta potential of carbon powders

The Zeta potential for PCFA and Kraft lignin carbon powders in deionized water are similar (Fig. 5), around -43.35 ± 0.48 mV and -42.05 ± 2.37 mV respectively. This suggests that the stability of the carbon particles obtained from PCFA is good enough to keep them in suspension for long durations. The Zeta value indicates repulsion between the particles, thus stopping them from attracting each other and flocculating. The low mobility and conductivity values (Table 4) indicate that the ionic double layer is thick due to low ionic strength. The mobility of the particles in the suspension,

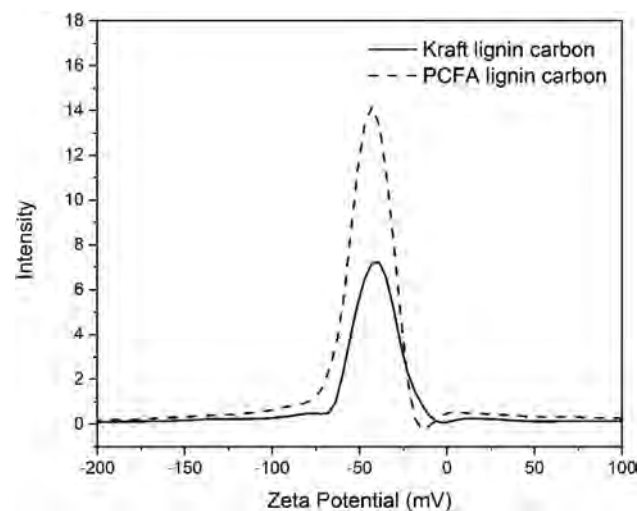


Fig. 5. Zeta potentials of carbon from carbonized fibers of Kraft and PCFA lignin.

$3.40\text{e-}004 \pm 00$ cm^2/V , indicates that the attraction of particles to the electrodes is very low. The higher ionic conductivity of Kraft lignin points to remnant impurities and complex sources of the originating liquid compared to that of PCFA.

3.4. Raman spectroscopy

Raman spectroscopy was performed to compare the purity of carbon obtained from PCFA and Kraft lignin powder samples. The deconvoluted spectra of carbonized fiber of Kraft lignin and PCFA are represented in Fig. 6A and B respectively. The spectra show the characteristic D band at about 1335 cm^{-1} for both lignins while the G band lies at about 1588 cm^{-1} for Kraft lignin carbon and 1512 cm^{-1} for PCFA. The D and G bands give the defect-derived structures and graphite derived structure of the carbon,

Table 4
Suspension properties of carbon from PCFA and Kraft lignin.

| Sample | Zeta potential (mV) | Mobility (cm^2/Vs) | Ionic conductivity (mS/cm) |
|--------------|------------------------|---|---|
| PCFA powder | -43.35 ± 0.48 | $3.40\text{e-}004 \pm 00$ | 0.028 ± 0.00042 |
| Kraft lignin | -42.05 ± 2.37 | $-3.1\text{e-}04 \pm 2.0\text{E-}06$ | 0.6457 ± 0.00051 |

respectively. The D band is due to the breathing modes of sp^2 atoms in the aromatic ring while the G band results from sp^2 site stretching of C=C bonds. A high G/D ratio is symptomatic of higher crystalline structure. Carbon from PAN has G/D ratios ranging from 0.57 to 0.67, while pitch-based carbon shows higher crystal perfection with G/D ratios ranging from 2.27 to 7.6 [57]. In deconvolution of spectra one more band is present at 1190 cm^{-1} for Kraft lignin carbon (Fig 6A) and at 1273 cm^{-1} for PCFA carbon (Fig 6B), referred to as the D4 band which represents ionic impurities and/or oxygen superficial group [58]. The intensity of G and D4 band are given relative to the total integrated in Table 5 along with the full width at half maximum of G (W_G) and D (W_D) band. The G-band intensity can also be used to check the purity of the samples; this is because, unlike with the D band, there is no effect of chirality on the G-band [59]. The width of the G and D bands corresponds to the structural disorder. Thus the Raman spectra show that high purity carbon obtained from PCFA is comparable to that obtained from PAN [60,61]. The highly ordered graphitic structure in PCFA-derived carbon is correlated with higher mechanical stiffness, thermal and electrical conductivity [577]. Kraft lignin carbon shows a higher value of W_D and lower intensity of the G band which indicates more structural disorder as compared to PCFA carbon. Thus, PCFA shows a higher carbon purity and structural order (see Fig. 6B).

3.5. Mechanical properties

Methods to measure the transverse and axial modulus of fibers having diameters of only a few microns are limited. Nano-indentation is one of the techniques that is being currently explored to effectively measure the mechanical properties of small dimensioned samples, especially carbon based fillers such as nanotubes and graphene [62]. Carbon fiber samples were embedded in epoxy resin and then polished for the axial and transverse measurements. Fig. 7 and Table 4 compare the axial and transverse modulus of the fibers from Kraft lignin and PCFA analyzed from the measurements shown in Fig. 7. It can be seen that the axial and transverse moduli of PCFA fibers are greater than those of Kraft lignin fibers. The elastic modulus of carbon fiber is correlated to the bond structure and strength [63], as well as to the percentage of graphitic molecular structure [577]. The Raman G/D ratio of 1.92 for PCFA as compared to 1.15 for Kraft lignin carbon (Table 5) is indicative of higher crystalline structure, consistent with the higher modulus values in both axial and transverse direction. The higher ratio of the axial to the transverse modulus of Kraft lignin fibers as compared to the PCFA fibers indicates that Kraft lignin is more aligned resulting in the lower transverse properties [64]. The higher carbon purity of PCFA is also a factor that could account for its improved mechanical properties. The properties of PCFA carbon fiber compare favorably with non bio-sourced carbon fibers prepared commercially. Determination of transverse properties of commercial carbon fibers by nano-indentation has been performed on M46J carbon fibers [65]; modulus was around 14 GPa. In a second study of the indentation of two PAN type commercial fibers, MK40 and MK46, the transverse moduli were measured as 15 ± 4.9 GPa and 14 ± 5.7 GPa respectively. In contrast, the value for a pitch based commercial fiber from Mitsubishi (Pitch K637) was shown to be 10.7 ± 3.1 GPa [64]. Gind-

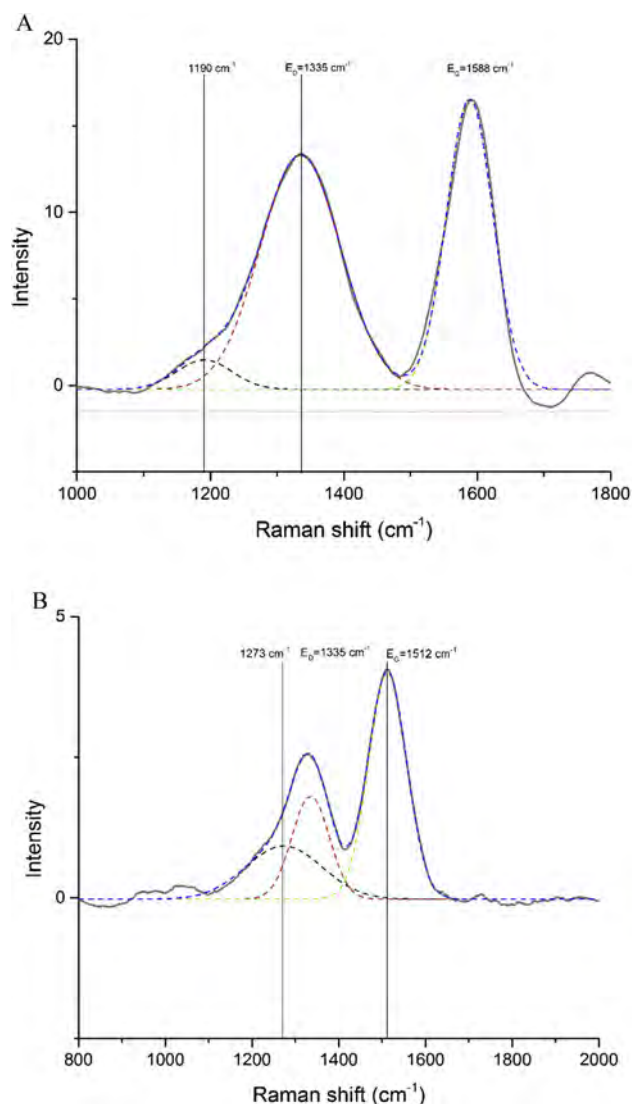


Fig. 6. Raman spectroscopy deconvoluted spectra of derived carbon (A) Kraft, (B) PCFA Lignin. (A color version of this figure can be viewed online.)

Altmutter et al. [66] performed nanoindentation of carbonized commercial Kraft lignin microparticles at $2000\text{ }^\circ\text{C}$, and reported the indentation modulus of 8.2 ± 3.04 GPa, higher than the modulus reported in Table 6 for Kraft lignin carbon (4.25 ± 0.82 GPa) which was carbonized at $900\text{ }^\circ\text{C}$. This can be explained by the higher temperature for carbonization leading to an increase in the graphitic structure causing an increase in crystallinity and modulus. Fan et al. reported the axial and transverse modulus of a commercial fiber T700SC using nanoindentation to be 23.17 ± 1.27 GPa and 1.81 ± 0.406 GPa [67]. The axial modulus is in the same range as that for both Kraft lignin and PCFA fibers, while the lower transverse modulus indicates lower alignment in PCFA carbon compared to the commercial T700SC fiber.

Table 5
Parameters obtained from deconvolution of Raman spectra of PCFA and Kraft lignin after carbonization.

| Sample | I_G/I_T (%) | I_D/I_T (%) | W_D (cm^{-1}) FWHM | W_G (cm^{-1}) FWHM |
|---------------------|---------------|-----------------------------|---------------------------------|---------------------------------|
| Kraft lignin carbon | 39.7 | 3.7 $\{I_{1190}/I_T\}$ (%) | 140.2 | 80.9 |
| PCFA carbon | 58.8 | 23.4 $\{I_{1273}/I_T\}$ (%) | 100.5 | 103.9 |

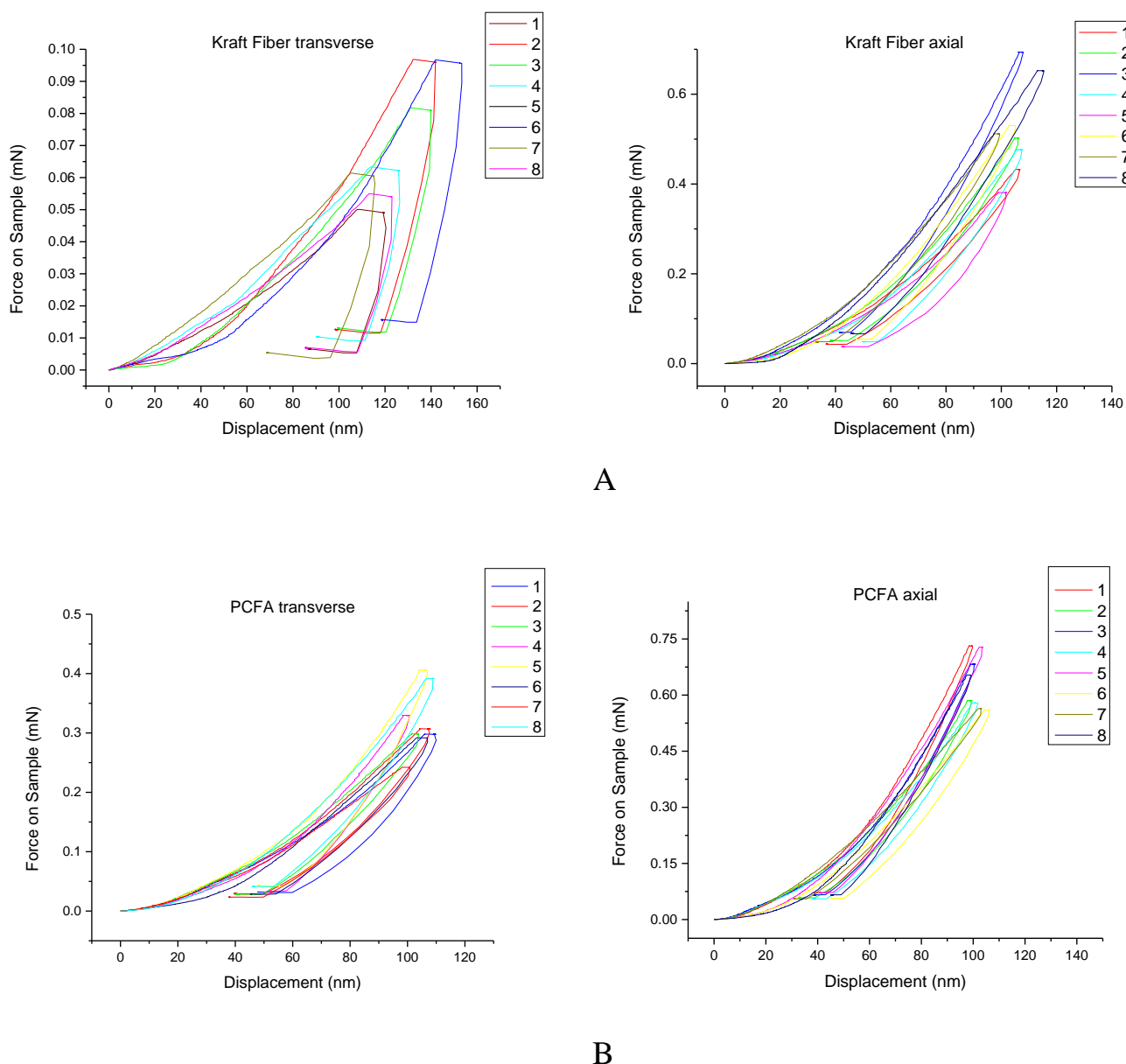


Fig. 7. Loading and depth curve of carbon fibers indented in transverse and axial axis derived from (A) Kraft, (B) PCFA lignins. (A color version of this figure can be viewed online.)

Table 6

Nanoindentation parameters of the carbon fiber.

| Sample | Modulus in transverse axis (GPa) | Modulus in axial axis (GPa) | Axial by transverse ratio |
|---------------------|----------------------------------|-----------------------------|---------------------------|
| Kraft lignin carbon | 4.25 ± 0.82 | 27.63 ± 5.01 | 6.5 |
| PCFA | 15.51 ± 0.78 | 34.52 ± 7.61 | 2.2 |

3.6. X-ray photoelectron spectroscopy (XPS)

XPS was performed to identify the state of chemical bonding of carbon in Kraft and PCFA fibers. First, a low resolution survey was performed to identify the percentage of carbon present on the surface. Table 7 lists all the main elements having atomic percent higher than 0.1. It shows PCFA containing more carbon percentage as compared to the Kraft carbon fiber.

High resolution C1s regions were analyzed to get the binding characteristics of the fiber surface. The deconvolution of the C1s

Table 7

Atomic percentage of the surface of carbon fibers using XPS.

| Sample | Element atomic (%) | | |
|--------------|--------------------|---------|----------|
| | C (at%) | O (at%) | Si (at%) |
| PCFA | 88.07 | 11.93 | – |
| Kraft carbon | 79.07 | 18.11 | 2.83 |

was performed using the PHI Multipak™ software. The background was subtracted using the Shirley method, while the peak

was fitted by Gauss-Lorentz mixed function. Fig. 8A and B represents the C1s curve fitting using Gauss-Lorentz function of Kraft and PCFA carbon fiber. Carbon was present in three states: the graphitic (C–C) peak at 284.3–284.7 eV, the ether (C–O) or hydroxyl group (C–OH) peak at 285.9–286.5 and the carbonyl or quinone group (C=O) at binding energy of 287.1–287.9 eV [68–70].

XPS results show a higher percentage of graphitic structure of carbon in PCFA as compared to Kraft lignin (Table 8). This is expected to correlate to better mechanical performance as the crystallinity of the structure reinforces the fiber leading to increased modulus. This is confirmed by the nanoindentation results. The graphitic peak for XPS also correlates to the G band intensity from the Raman spectroscopy which shows a similar trend.

3.7. Transmission electron microscopy (TEM)

The TEM image and corresponding SAD ring pattern images for Kraft and PCFA carbon fibers are shown in Fig. 9A and B

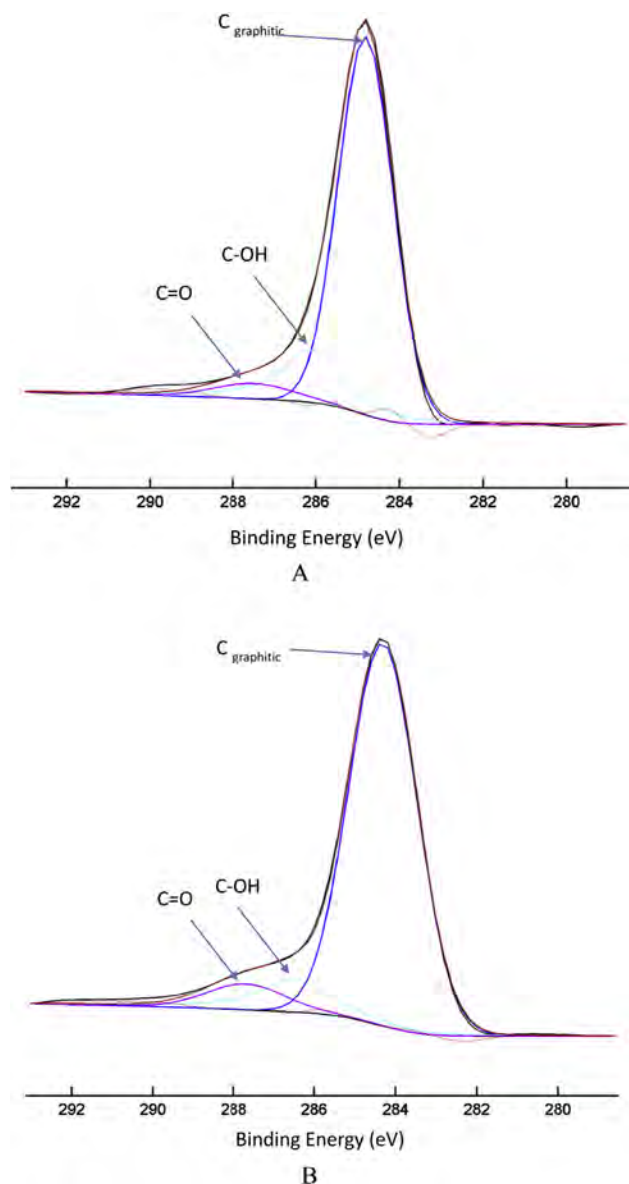


Fig. 8. Deconvolution of C 1s region of (A) Kraft (B) PCFA carbon fiber. (A color version of this figure can be viewed online.)

Table 8

Deconvolution of C 1s region for the Kraft and PCFA carbon fiber.

| Sample | Graphite (C–C) | | C–O | | C=O | |
|--------|----------------|-------|---------|-------|---------|------|
| | BE (eV) | M(%) | BE (eV) | M(%) | BE (eV) | M(%) |
| Kraft | 284.7 | 73.16 | 285.9 | 23.47 | 287.1 | 3.37 |
| PCFA | 284.3 | 81.43 | 286.5 | 13.46 | 287.9 | 5.11 |

respectively. Both consist of multi crystals according to the diffraction rings. There is a difference in the crystal dimensions. Kraft lignin has a smaller crystallite as compared to the PCFA. A small crystal dimension enhances tensile strength [71] whereas a large crystal enhances the stiffness and modulus of the fibers [72]. This correlates to the nanoindentation results of PCFA having higher modulus.

3.8. XRD

From the diffraction pattern (Fig. 10A and B), one can observe that both the Kraft and PCFA fibers show reflections at (002) and (001) plane characteristic of carbon fibers from plant sources [73]. The broader peak of (002) observed for Kraft lignin carbon fiber is indicative of a large number of small crystallites present in the fiber. Ring diffraction pattern from TEM also shows a large number of crystallites for Kraft lignin. The narrow peak and higher intensity of the (002) peak for PCFA shows higher crystallinity for PCFA fibers. The lattice parameter was calculated using Bragg's law and apparent crystallite thickness (L_c) was calculated using the Scherrer formula reported in Table 9. Both the fibers are in between turbostratic and graphitic structure, PCFA tends more towards graphitic structure as observe from degree of graphitization value. These results indicate that the PCFA has a more orderly arrangement of carbon atoms as compared to the Kraft.

3.9. Thermogravimetric analysis (TGA)

TGA was used to assess the thermal stabilities of the obtained CFs. Fig. 11 compares the TGA curves of Kraft and PCFA CFs up to 800 °C and the residual weights. PCFA demonstrated good thermal stability as compared to Kraft carbon fiber having 59.8% residual weight as compared to the 16.7% for Kraft lignin carbon fiber at 800 °C (Table 10). The weight loss observed below 100 °C mainly in PCFA may be due to the moisture absorbed on the surface of the fiber as noted by others [74]. The weight loss from 100 °C to 400 °C may be because of labile oxygen containing groups present in the material [75]. Both fibers show some stability until 400 °C. There is a sudden decrease in weight for Kraft carbon and PCFA at temperature around 450 °C similar to that reported by Xu et al. [47] as T_{onset} for carbon fiber from a 50:50 lignin/PAN source. This can be due to the removal of more stable oxygen functionalities [76]. PCFA seems more stable over the temperature range which is comparable to the carbonized lignin/PAN fiber thermal stability shown by Xu et al. [47]. The residual is 76.1% wt. at 700 °C as compared to 67.9% for PCFA at the same temperature.

4. Conclusions

In this work we have reported the formation of PCFA-based carbon fiber, and compared its properties to those of fibers derived from Kraft lignin. Kraft-lignin had a higher molecular weight than PCFA, and the percentage of carbon in the Kraft lignin was higher than in PCFA prior to pyrolysis. Notable to our approach is that the fibers were successfully electrospun directly from solution without any chemical treatment or addition of polymers to

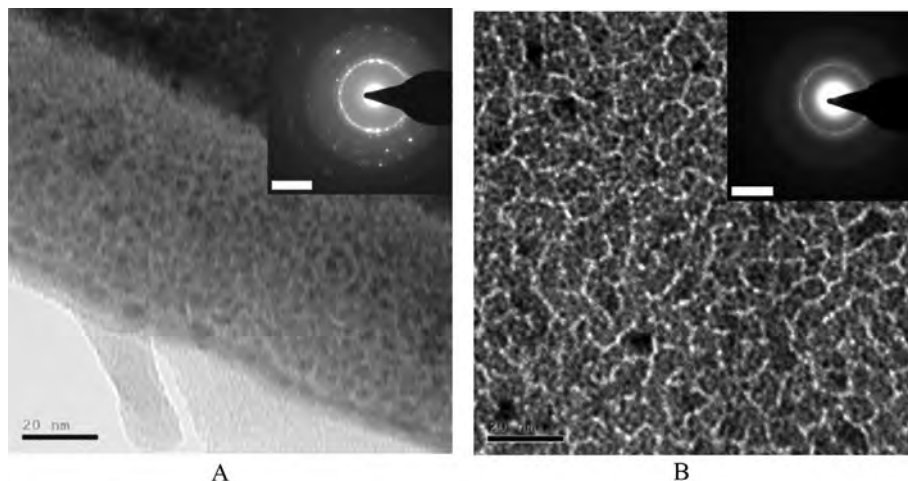


Fig. 9. TEM and electronic diffraction image of (A) Kraft (B) PCFA carbon fiber.

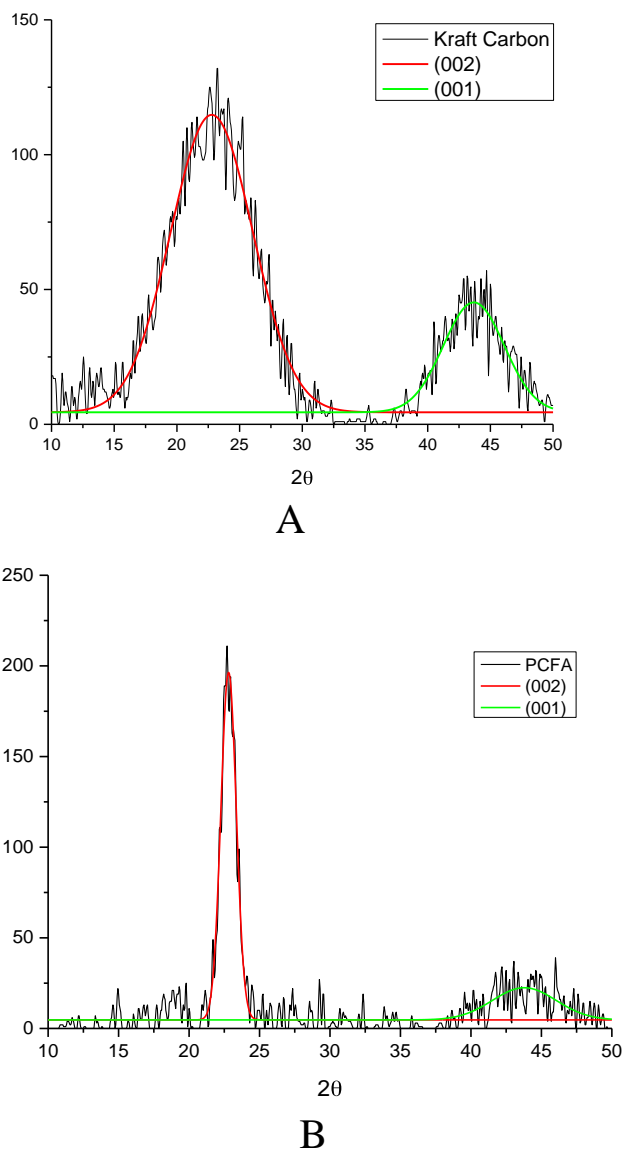


Fig. 10. X-ray diffraction pattern of (A) Kraft (B) PCFA carbon fiber. (A color version of this figure can be viewed online.)

Table 9
Structure parameters of X-ray diffraction of Kraft and PCFA carbon fiber.

| Sample | $d_{(002)}$ (nm) | $d_{(001)}$ (nm) | L_c (nm) | g(%) |
|---------------------|------------------|------------------|------------|-------|
| Kraft lignin carbon | 0.391 | 0.207 | 2.07 | −5.46 |
| PCFA | 0.389 | 0.206 | 12.28 | −5.23 |

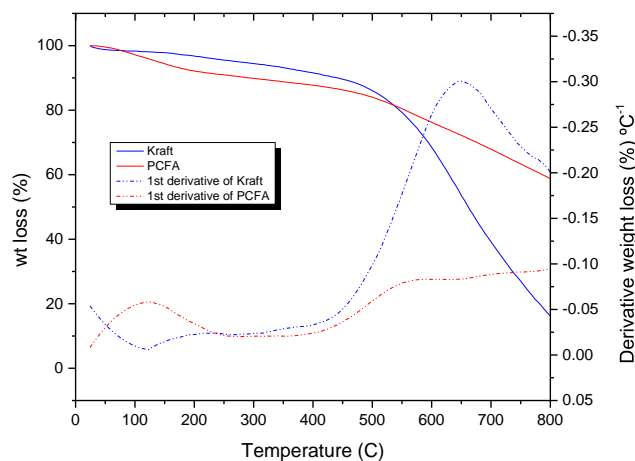


Fig. 11. TGA curve and 1st derivative of Kraft and PCFA carbon fiber. (A color version of this figure can be viewed online.)

Table 10
Residue weights of Kraft and PCFA carbon fibers at different temperatures determined by TGA.

| Sample | Residue weight (wt.%) | | |
|--------|-----------------------|--------|--------|
| | 400 °C | 600 °C | 800 °C |
| PCFA | 87.7 | 76.2 | 59.8 |
| Kraft | 91.4 | 68.3 | 16.7 |

provide fiber extensional flow strength. Kraft lignin in the unmodified state (no coaxial die with ethanol coating or blended polymers used by others to produce sub-micron Kraft fibers) produced fibers that were of high diameter (~50 μm). In contrast, the PCFA-sourced carbon fibers were of low diameter (~10 μm). Carbonization at 900 °C imparted more graphitic properties to the PCFA carbon than to the Kraft lignin, as seen from G/D ratios of 1.92

vs 1.15 respectively. In this respect, the PCFA-derived carbon compares very well to commercial carbon from PAN and approaches that based on pitch. The carbon content is around 86% for both lignin bio-sources of carbon based on elemental analysis. Higher G band peaks are associated with both crystal perfection and low impurities. Nanoindentation results showed that the carbon from PCFA and Kraft had comparable axial moduli compared to commercial carbon. The transverse moduli of the PCFA was better than Kraft and commercial carbon fibers. XPS results show 88% graphitic C–C bond for PCFA as compared to 79% for the Kraft lignin indicating higher crystallinity, which can be correlated to high G/D Raman ratio for PCFA. Moreover, from the XRD and TEM a larger crystal size for the PCFA fiber was obtained which correlates to the higher nanoindentation modulus of the fiber. TGA curves also show higher thermal stability for PCFA indicating higher graphitization. The higher impurities in Kraft lignin were reflected in the zeta potential higher ionic conductivity and lower mobility compared to PCFA carbon. The carbon from both lignin showed good dispersion stability in DI water. On the basis of our results, PCFA appears to be a promising new renewable source of both carbon fibers and pure carbon. The subject of our further research will be to shift PCFA lignin extraction to green chemistry by applying steam explosion combined with enzymatic hydrolysis.

Acknowledgments

NAD, RAD and FC acknowledge NSF 1456286. NAD acknowledges support from NSF CMMI 1031828 and NSF PFI 1114389. RAD and FC acknowledge support from the US Department of Energy's Bioenergy Sciences Center, supported by the Office of Biological and Environmental Research in the DOE Office of Science (BER DE-AC05-00OR22725). We thank Dr Daphna Havkin-Frenkel, Bakto Flavors LLC, for provision of *V. planifolia* seeds. We thank Reza Mirshams, UNT for access to the Nanoindentation instrument.

References

- [1] G. Williams, R. Trask, I. Bond, A self-healing carbon fibre reinforced polymer for aerospace applications, *Compos. Part A Appl. Sci. Manuf.* 38 (6) (June 2007) 1525–1532.
- [2] S.B. Sastri, J.P. Armistead, T.M. Keller, Phthalonitrile-carbon fiber composites, *Polym. Compos.* 17 (1996) 816–822, <http://dx.doi.org/10.1002/pol.10674>.
- [3] D.D.L. Chung, Electromagnetic interference shielding effectiveness of carbon materials, *Carbon* 39 (2) (February 2001) 279–285.
- [4] Naoto Saito, Kaoru Aoki, Yuki Usui, Masayuki Shimizu, Kazuo Hara, Nobuyo Narita, Nobuhide Ogihara, Koichi Nakamura, Norio Ishigaki, Hiroyuki Kato, Hisao Haniu, c Seiichi Taruta, d Yoong Ahm Kimd, Morinobu Endod, Application of carbon fibers to biomaterials: a new era of nano-level control of carbon fibers after 30-years of development, *Chem. Soc. Rev.* 40 (2011) 3824–3834.
- [5] James F. Snyder, Emma L. Wong, Clifford W. Hubbard, Evaluation of commercially available carbon fibers, fabrics, and papers for potential use in multifunctional energy storage applications, *J. Electrochem. Soc.* 156 (2009) A215–A224.
- [6] Marcus Rose, Emanuel Kockrick, Irena Senkovska, Stefan Kaskel, High surface area carbide-derived carbon fibers produced by electrospinning of polycarbosilane precursors, *Carbon* 48 (2) (February 2010) 403–407.
- [7] V.B. Fedorov, M. Kh Shorosov, D.K. Khakimova, Carbon and its Reactions with Metals, Metallurgiya, Moscow, 1978.
- [8] M. Minus, S. Kumar, The processing, properties, and structure of carbon fibers, *Jom* 57 (2) (2005) 52–58.
- [9] Z. Wangxi, L. Jie, W. Gang, Evolution of structure and properties of PAN precursors during their conversion to carbon fibers, *Carbon* 41 (14) (2003) 2805–2812.
- [10] M.S.A. Rahaman, A.F. Ismail, A. Mustafa, A review of heat treatment on polyacrylonitrile fiber, *Polym. Degrad. Stab.* 92 (8) (2007) 1421–1432.
- [11] A. Mavinkurve, S. Visser, A.J. Pennings, An initial evaluation of poly(vinylacetylene) as a carbon fiber precursor, *Carbon* 33 (6) (1995) 757–761.
- [12] Horikiri, S., Iseki, J., and Minobe, M. (1978). U.S. Patent No. 4,070,446. Washington, DC: U.S. Patent and Trademark Office.
- [13] J.A. Newell, D.D. Edie, Factors limiting the tensile strength of PBO-based carbon fibers, *Carbon* 34 (5) (1996) 551–560.
- [14] Jason Hilla, Stephen Polaskya, Erik Nelsonc, David Tilmanb, Hong Huod, Lindsay Ludwige, James Neumann, Haochi Zhenga, Diego Bontaa, Climate change and health costs of air emissions from biofuels and gasoline, *PNAS* 106 (6) (February 10, 2009) 2077–2082.
- [15] A.L. Compere, W.L. Griffith, C.F. Leitten, J.T. Shaffer, Low cost carbon fiber from renewable resources, in: *International SAMPE Technical Conference*, vol. 33, 2001, August, pp. 1306–1314.
- [16] A.J. Ragauskas, G.T. Beckham, M.J. Biddy, R. Chandra, F. Chen, M.F. Davis, B.H. Davison, R.A. Dixon, P. Gilna, M. Keller, P. Langan, A.K. Naskar, J.N. Saddler, T.J. Tschaplinski, G.A. Tuskan, C.E. Wyman, Lignin valorization: improving lignin processing in the biorefinery, *Science* 344 (2014) 709.
- [17] F. Chen, R.A. Dixon, Lignin modification improves fermentable sugar yields for biofuel production, *Nat. Biotechnol.* 25 (2007) 759–761.
- [18] M.S.S. Reddy, F. Chen, G.L. Shadle, L. Jackson, R.A. Dixon, Targeted down-regulation of cytochrome P450 enzymes for forage quality improvement in alfalfa (*Medicago sativa* L.), *Proc. Natl. Acad. Sci. U. S. A.* 102 (2005) 16573–16578.
- [19] R. Vanholme, K. Morreel, C. Darrah, P. Oyarce, J.H. Grabber, J. Ralph, W. Boerjan, Metabolic engineering of novel lignin in biomass crops, *New Phytol.* 196 (2012) 978–1000.
- [20] Y. Tsuji, R. Vanholme, Y. Tobimatsu, Y. Ishikawa, C.E. Foster, N. Kamimura, et al., Introduction of chemically labile substructures into arabidopsis lignin through the use of LigD, the C α -dehydrogenase from *spingobium* sp. strain SYK-6, *Plant Biotechnol. J.* 13 (6) (2015) 821–832, <http://dx.doi.org/10.1111/pbi.12316>.
- [21] E. Sjöström, *Wood Chemistry: Fundamentals and Application*, Academic Press, Orlando, 1993, p. 293.
- [22] I.W. Pearl, *The Chemistry of Lignin*, Marcel Dekker, Inc., New York, 1967, p. 339.
- [23] W. Boerjan, J. Ralph, M. Baucher, Lignin biosynthesis, *Annu. Rev. Plant Biol.* 54 (2003) 519–546.
- [24] J. Ralph, K. Lundquist, G. Brunow, F. Lu, H. Kim, P.F. Schatz, J.M. Marita, R.D. Hatfield, S. a. Ralph, J.H. Christensen, W. Boerjan, Lignins: natural polymers from oxidative coupling of 4-hydroxyphenyl- propanoids, *Phytochem. Rev.* 3 (2004) 29–60.
- [25] R.A. Patil, Cleavage of Acetyl Groups of Acetic Acid Production in Kraft Pulp Mills, Thesis, University of Maine, 2012.
- [26] L.S. Kocheva, A.P. Karmanov, M.V. Mironov, V.A. Belyi, V.Y. Belyaev, Y.B. Monakov, Straw lignins: Hydrodynamic and conformational properties of the macromolecules, *Russ. J. Appl. Chem.* 81 (2008) 2033–2039.
- [27] F. Chen, Y. Tobimatsu, D. Havkin-Frenkel, R.A. Dixon, J. Ralph, A polymer of caffeyl alcohol in plant seeds, in: *Proceedings of the National Academy of Sciences USA* 109, 2012, pp. 1772–1777.
- [28] F. Chen, Y. Tobimatsu, L. Jackson, J. Ralph, R.A. Dixon, Novel seed coat lignins in the Cactaceae: structure, distribution and implications for the evolution of lignin diversity, *Plant J.* 73 (2013) 201–211.
- [29] Y. Tobimatsu, F. Chen, J. Nakashima, L.A. Jackson, R.A. Dixon, J. Ralph, Coexistence but independent biosynthesis of catechyl and guaiaacyl/syringyl lignins in plant seeds, *Plant Cell* 25 (2013) 2587–2600.
- [30] V.K. Thakur, M.K. Thakur, P. Raghavan, M.R. Kessler, Progress in green polymer composites from lignin for multifunctional applications: a review, *ACS Sustain. Chem. Eng.* 2 (5) (2014) 1072–1092, <http://dx.doi.org/10.1021/sc500087z>.
- [31] D.A. Baker, N.C. Gallego, F.S. Baker, On the Characterization and spinning of an organic purified lignin toward the manufacture of low-cost carbon fiber, *J. Appl. Polym. Sci.* 124 (2012) 227–234.
- [32] Otani, S.; Fukuoka, Y.; Igarashi, B.; Sasaki, K. US Pat. 3,461,082, 1969, FR Pat. 1,458,725, (1966).
- [33] K. Sudo, Shimizu, A new carbon fiber from lignin, *J. Appl. Polym. Sci.* 44 (1992) 127–134.
- [34] K. Sudo, K. Shimizu, N. Nakashima, A. Yokoyama, A new modification method of exploded lignin for the preparation of a carbon fiber precursor, *J. Appl. Polym. Sci.* 48 (1993) 1485–1491.
- [35] Y. Uraki, S. Kubo, N. Nigo, et al., Preparation of carbon fibers from organosolv lignin obtained by aqueous acetic acid pulping, *Holzforsch. Int. J. Biol. Chem. Phys. Technol. Wood* 49.4 (2009) 343–350.
- [36] S. Kubo, Y. Uraki, Y. Sano, Preparation of carbon fibers from softwood lignin by atmospheric acetic acid pulping, *Carbon* 36 (7–8) (1998) 1119–1124.
- [37] C. Mai, A. Majcherzyk, A. Hüttermann, Chemo-enzymatic synthesis and characterization of graft copolymers from lignin and acrylic compounds, *Enzyme Microb. Technol.* 27 (2000) 167–175.
- [38] B. Xiao, X.F. Sun, R.C. Sun, The chemical modification of lignins with succinic anhydride in aqueous systems, *Polym. Degrad. Stab.* 71 (2) (2001) 223–231.
- [39] M. Lallave, J. Bedia, R. Ruiz-Rosas, J. Rodriguez-Mirasol, T. Cordero, J.C. Otero, M. Marquez, A. Barrero, I.J.G. Loscertales, Filled and hollow carbon nanofibers by coaxial electrospinning of allcell lignin without binder, *Polymers* 19 (23) (29 NOV 2007). Article first published online.
- [40] J.F. Kadla, s Kubo, R.D. Gilbert, R.A. Venditti, A.L. Compere, W.L. Griffith, Lignin-based carbon fibers for composite fiber applications, *Carbon* 40 (2002) 2913–2920.
- [41] S. Kubo, J.F. Kadla, Kraft lignin/poly(ethylene oxide) blends: effect of lignin structure on miscibility and hydrogen bonding, *J. Appl. Polym. Sci.* 98 (2005) 1437–1444.
- [42] Satoshi Kubo, John F. Kadla, Poly(ethylene oxide)/organosolv lignin blends: Relationship between thermal properties, Chem. Struct. Blend Behav. *Macromol.* 37 (2004) 6904–6911.

- [43] S. Kubo, J.F. Kadla, Lignin-based carbon fibers: effect of synthetic polymer blending on fiber properties, *J. Polym. Environ.* 13 (No. 2) (April 2005).
- [44] Jian Lin, Satoshi Kubo, Tatsuhiko Yamada, Keiichi Koda, Yasumitsu Urak, Chemical thermostabilization for the preparation of carbon fibers from softwood lignin, *BioResources* 7 (4) (2012) 5634–5646.
- [45] Mariko Ago, Kunihiko Okajima, Joseph E. Jakes, Sunkyu Park, Orlando J. Rojas, Lignin-based electrospun nanofibers reinforced with cellulose nanocrystals, *Biomacromolecules* 13 (3) (2012) 918–926.
- [46] D.K. Seo, J.P. Jeun, H.B. Kim, P.H. Kang, Preparation and characterization of the carbon nanofibers mat produced from electrospun PAN/lignin precursors by electron beam irradiation, *Rev. Adv. Mater. Sci.* 28 (2011) 31–34.
- [47] X. Xu, J. Zhou, L. Jiang, G. Lubineau, S.A. Payne, D. Gutschmidt, Lignin-based carbon fibers: carbon nanotube decoration and superior thermal stability, *Carbon* 80 (2014) 91–102.
- [48] W.G. Glasser, V. Davé, C.E. Frazier, Molecular weight distribution of (semi-) commercial lignin derivatives, *J. Wood Chem. Technol.* 13 (4) (1993) 545–559.
- [49] I. Norberg, Y. Nordström, R. Drougge, G. Gellerstedt, E. Sjöholm, A new method for stabilizing softwood Kraft lignin fibers for carbon fiber production, *J. Appl. Polym. Sci.* (2013) 38588.
- [50] X. Li, B. Bhushan, A review of nanoindentation continuous stiffness measurement technique and its applications, *Mater. Character.* 48 (2002) 11–36.
- [51] W.C. Oliver, G.M. Pharr, An improved technique for determining hardness and elastic modulus using load and displacement sensing indentation experiments, *J. Mater. Res.* 7 (6) (June 1992) 1564–1583.
- [52] J.L. Hay, G.M. Pharr, Instrumented indentation testing, in: *ASM Handbook, Mechanical Testing and Evaluation*, vol. 8, October 2000, pp. 232–243.
- [53] X. Pan, Y. Sano, Fractionation of wheat straw by atmospheric acetic acid process, *Bioresour. Technol.* 96 (11) (2005) 1256–1263.
- [54] A.K. Bledzki, V.E. Sperber, O. Faruk, Structure and Chemical Constituents of fibres, in: *Natural and Wood Fibre Reinforcement in Polymers*, Rapra Review Reports 13 (8), Rapra Technology Limited, Shawbury, United Kingdom, 2002, p. 12.
- [55] A.U. Buranov, G. Mazza, Lignin in straw of herbaceous crops, *Ind. Crops Prod.* 28 (2008) 237–259.
- [56] S. Manandhar, S. Vidhate, N.A. D'Souza, Water soluble levan polysaccharide biopolymer electrospun fibers, *Carbohydr. Polym.* 78 (2009) 794–798.
- [57] H.O. Pierson, *Handbook of Carbon, Graphite, Diamond and Fullerenes: Properties, Processing and Applications*, Noyes Publications, 1993.
- [58] R. Ruiz-Rosas, J. Bedía, M. Lallave, I.G. Loscertales, A. Barrero, J. Rodríguez-Mirasol, T. Cordero, The production of submicron diameter carbon fibers by the electrospinning of lignin, *Carbon* 48 (3) (2010) 696–705. <http://dx.doi.org/10.1016/j.carbon.2009.10.014>.
- [59] K.K. Kim, J.S. Park, S.J. Kim, et al., Dependence of Raman spectra G₂ band intensity on metallicity of single-wall carbon nanotubes, *Phys. Rev. B* 76 (20) (2007). Article ID 205426.
- [60] D. Ramani Venugopalan, R. Sathiyamoorthy, A.K. Acharya, Tyagi, Neutron irradiation studies on low density pan fiber based carbon/carbon composites, *J. Nucl. Mater.* 404 (2010) 19–24.
- [61] Zhiqiang Maa, Ekaterina Troussard, Jeroen A. van Bokhoven, Controlling the selectivity to chemicals from lignin via catalytic fast pyrolysis, *Appl. Catal. A Gen.* 423–424 (2012) 130–136.
- [62] Ana M. Díez-Pascual, Marián A. Gómez-Fatou, Fernando Ania, Araceli Flores, Nanoindentation in polymer nanocomposites, *Prog. Mater. Sci.* 67 (2015) 1–94 (0) (1).
- [63] R. Longtin, C. Fauteux, E. Coronel, U. Wiklund, J. Pegna, M. Boman, Nano-indentation of carbon microfibers deposited by laser-assisted chemical vapor deposition, *Appl. Phys. A* 79 (3) (2004) 573–577.
- [64] R. Maurin, P. Davies, N. Baral, C. Baley, Transverse properties of carbon fibres by nano-indentation and micro-mechanics, *Appl. Comp. Mater.* 15 (2008) 61–73.
- [65] Mickey G. Huson, Jeffrey S. Church, Abdullah A. Kafi, Andrea L. Woodhead, Ji Yi Khoo, M.S.R.N. Kiran, Jodie C. Bradby, Bronwyn L. Fox, Heterogeneity of carbon fibre, *Carbon* 68 (2014) 240–249 (0) (3).
- [66] Wolfgang Gindl-Altmutter, Fürst Christian, raj Mahendran Arunjunai, Obersriebnig Michael, Emsenhuber Gerhard, Kluge Marcel, Veigel Stefan, Keckes Jozef, Liebner Falk, Electrically conductive Kraft lignin-based carbon filler for polymers, *Carbon* 89 (2015) 161–168 (0) (8).
- [67] Zheqiong Fan, Ruixuan Tan, Kejian He, Mingyu Zhang, Wangshu Peng, Qizhong Huang, Preparation and mechanical properties of carbon fibers with isotropic pyrolytic carbon core by chemical vapor deposition, *Chem. Eng. J.* 272 (2015) (0) (7/15): 12–6.
- [68] M.C. Paiva, C.A. Bernardo, M. Nardin, Mechanical, surface and interfacial characterisation of pitch and PAN-based carbon fibres, *Carbon* 38 (9) (2000) 1323–1337. [http://dx.doi.org/10.1016/S0008-6223\(99\)00266-3](http://dx.doi.org/10.1016/S0008-6223(99)00266-3).
- [69] J. Wang, F. Zhao, Y. Hu, R. Zhao, R. Liu, Modification of activated carbon fiber by loading metals and their performance on SO₂ removal, *Chin. J. Chem. Eng.* 14 (4) (2006) 478–485. [http://dx.doi.org/10.1016/S1004-9541\(06\)60102-X](http://dx.doi.org/10.1016/S1004-9541(06)60102-X).
- [70] Ida Brodin, Marie Ernstsson, Göran Gellerstedt, Elisabeth Sjöholm, Oxidative stabilisation of Kraft lignin for carbon fibre production, *Holzforschung* 66 (2) (2011) 141–147. <http://dx.doi.org/10.1515/HF.2011.133>.
- [71] H.E. Dongxin, W.A.N.G. Chengguo, B.A.I. Yujun, et al., Comparison of structure and properties among various PAN fibers for carbon fibers, *J. Mater. Sci. Technol.* 21 (03) (2005) 376–380.
- [72] Y. Termonia, Chapter 11-molecular modeling of the stress/strain behavior of spider dragline, *Pergamon. Mater. Ser.* 4 (2000) 337–349. [http://dx.doi.org/10.1016/S1470-1804\(00\)80015-2](http://dx.doi.org/10.1016/S1470-1804(00)80015-2).
- [73] X. Ma, C. Yuan, X. Liu, Mechanical, microstructure and surface characterizations of carbon fibers prepared from cellulose after liquefying and curing, *Materials* 7 (2014) 75–84.
- [74] X. Yang, X. Zhang, Y. Ma, Y. Huang, Y. Wang, Y. Chen, Superparamagnetic graphene oxide-Fe₃O₄ nanoparticles hybrid for controlled targeted drug carriers, *J. Mater. Chem.* 19 (18) (2009) 2710–2714. <http://dx.doi.org/10.1039/B821416F>.
- [75] X. Tang, B. Yu, R.V. Hansen, X. Chen, X. Hu, J. Yang, Grafting low contents of branched polyethylenimine onto carbon fibers to effectively improve their interfacial shear strength with an epoxy matrix, *Adv. Mater. Interfaces* 2 (12) (2015). <http://dx.doi.org/10.1002/admi.201500122> n/a-n/a.
- [76] J. Shen, B. Yan, T. Li, Y. Long, N. Li, M. Ye, Mechanical, thermal and swelling properties of poly(acrylic acid)-graphene oxide composite hydrogels, *R. Soc. Chem.* (2012). <http://dx.doi.org/10.1039/C1SM06970E>.